Hindawi
Advances in Mathematical Physics
Volume 2018, Article ID 2365602, 12 pages
https://doi.org/10.1155/2018/2365602

Research Article

Statistics of Finite Scale Local Lyapunov Exponents in Fully Developed Homogeneous Isotropic Turbulence

Nicola de Divitiis

"La Sapienza" University, Dipartimento di Ingegneria Meccanica e Aerospaziale, Via Eudossiana, 18, 00184 Rome, Italy

Correspondence should be addressed to Nicola de Divitiis; n.dedivitiis@gmail.com

Received 21 February 2018; Accepted 2 May 2018; Published 6 June 2018

Academic Editor: Xavier Leoncini

The present work analyzes the statistics of finite scale local Lyapunov exponents of pairs of fluid particles trajectories in fully developed incompressible homogeneous isotropic turbulence. According to the hypothesis of fully developed chaos, this statistics is here analyzed assuming that the entropy associated with the fluid kinematic state is maximum. The distribution of the local Lyapunov exponents results in an unsymmetrical uniform function in a proper interval of variation. From this PDF, we determine the relationship between average and maximum Lyapunov exponents and the longitudinal velocity correlation function. This link, which in turn leads to the closure of von Kármán–Howarth and Corrsin equations, agrees with results of previous works, supporting the proposed PDF calculation, at least for the purposes of the energy cascade main effect estimation. Furthermore, through the property that the Lyapunov vectors tend to align the direction of the maximum growth rate of trajectories distance, we obtain the link between maximum and average Lyapunov exponents in line with the previous results. To validate the proposed theoretical results, we present different numerical simulations whose results justify the hypotheses of the present analysis.

1. Introduction

In fully developed turbulence, the finite scale Lyapunov exponents of the fluid kinematic field are of paramount importance because they (i) describe the turbulent energy cascade phenomenon and (ii) give the fluid viscous dissipation when the length scale goes to zero. One of the characteristics of these exponents in turbulence is that their statistics is related to the instantaneous velocity field, whereas they do not depend directly on the time variations of this latter. Such characteristic, which represents the crucial point of this work, is consequence of the fact that the times of variations of the velocity field, which changes according to the Navier–Stokes equations, are much greater than those of the fluid displacements which follow the fluid kinematics [1, 2]. Specifically, whereas the velocity field is a function of slow growth of the time, the distance between particles and the local fluid deformation are unbounded quantities which rise exponentially with the time [1]. Accordingly, the fluid particles displacements statistics, being not directly linked to the time variations of the velocity field, can be considered to be the result of the current fluid act of motion.

It is worth remarking that the adoption of the finite scale Lyapunov exponents in place of the classical ones is justified by the fact that the turbulence is a complex phenomenon involving numerous length scales; each of them is characterized by different properties. The several perturbations of finite size will vary following nonlinear differential equations out of tangent space; thus the sole use of classical Lyapunov exponents is not adequate to describe the perturbations behavior associated with the different length scales and therefore the energy cascade.

Next, as a result of item (i), the knowledge of the Lyapunov exponents statistics would lead to the closure of the equations of velocity and temperature correlations and therefore to the determination of kinetic energy and temperature spectra. Therefore, the distribution of such exponents is very important for quantifying the effects of the turbulent energy cascade.

Several works dealing with the closure of the correlations equations are present in the literature, for instance, [3–9]. Nevertheless, to the author's knowledge, the influence of the finite scale Lyapunov exponents statistics on turbulent energy cascade and on the closure of the correlations equations

has not received due attention. Hence, the objective of the present work is to develop a theoretical analysis based on the aforementioned properties which leads to determining the statistics of the local finite scale Lyapunov exponent in fully developed homogeneous isotropic turbulence for incompressible fluids. This local exponent defined as

$$\widetilde{\lambda} \equiv \frac{d \ln \rho}{dt} = \frac{\dot{\boldsymbol{\xi}} \cdot \boldsymbol{\xi}}{\boldsymbol{\xi} \cdot \boldsymbol{\xi}} \tag{1}$$

provides the instantaneous growth rate of the distance $\rho = \sqrt{\boldsymbol{\xi} \cdot \boldsymbol{\xi}}$ between two fluid particles trajectories $\mathbf{x}(t)$ and $\mathbf{y}(t) = \mathbf{x}(t) + \boldsymbol{\xi}(t)$, where $\boldsymbol{\xi}$ is the separation vector (finite scale Lyapunov vector). This exponent is linked to the so called finite size Lyapunov exponent, FSLE, defined in [10] in a more general framework of dynamic systems. Specifically, FSLE can be obtained in terms of $\widetilde{\lambda}$ as a proper average of $\widetilde{\lambda}$ over a given interval, say $T = \sum_k (t_k - t_{k-1})$, where (t_k, t_{k-1}) is the subset in which ρ rises from $\rho(t_{k-1})$ to $\varrho_R \rho(t_{k-1})$, $\varrho_R > 1$ is an assigned threshold slightly greater than the unity to avoid interferences between the scales, and $\boldsymbol{\xi}(t_k)$, $k = 1, 2, \ldots$, are rescaled along the direction $\boldsymbol{\xi}(t_k)/|\boldsymbol{\xi}(t_k)|$.

Because of nonsmooth spatial variations of the velocity field, $\widetilde{\lambda}$ can exhibit fluctuations of sizable amplitude with respect to its average value; thus $\widetilde{\lambda}$ plays the role of a stochastic variable and will be distributed according to a certain PDF. To define the magnitude of these oscillations, average and maximum finite scale Lyapunov exponents, $\overline{\lambda}$ and λ_+ respectively, are defined as

$$\begin{aligned} \overline{\lambda} &\equiv \left\langle \widetilde{\lambda} \right\rangle, \\ \lambda_+ &\equiv \left\langle \widetilde{\lambda} \right\rangle_{\dot{\xi} \cdot \xi \geq 0}, \end{aligned} \tag{2}$$

where $\langle \circ \rangle$ and $\langle \circ \rangle_{\dot{\xi} \cdot \xi \geq 0}$ denote the average over the entire ensemble of $\boldsymbol{\xi}$ and the average calculated on the ensemble where $\dot{\boldsymbol{\xi}} \cdot \boldsymbol{\xi} \geq 0$.

As a consequence of the aforementioned properties, the present analysis assumes that the kinematics of a pair of fluid particles, characterized by $\boldsymbol{\xi}$, is much faster and statistically independent with respect to the time variations of velocity field. This property, just discussed in [1, 2] for what concerns the closure of von Kármán–Howarth and Corrsin equations [11–13], was previously supported by the arguments presented in [14] (and references therein), where the author observes the following: (i) the velocity fields $\mathbf{u}(t, \mathbf{x})$ produce chaotic trajectories also for relatively simple mathematical structure of $\mathbf{u}(t, \mathbf{x})$; (ii) the flows given by $\mathbf{u}(t, \mathbf{x})$ stretch and fold continuously and rapidly causing an effective mixing of the particles trajectories.

Through the hypotheses of fully developed chaos and fluid incompressibility, we first estimate the interval of variation of $\widetilde{\lambda}$ and thereafter determine the distribution function of $\widetilde{\lambda}$ by maximizing the entropy associated with the fluid kinematic state. The maximization of such entropy is justified by the fact that the regime of fully developed turbulence corresponds to a situation of maximum chaos where the bifurcations cause a total loss of the initial condition data of $\mathbf{x}$ and $\boldsymbol{\xi}$. As a consequence, we show that $\widetilde{\lambda}$ will be uniformly distributed in such interval; in particular, we determine the relationship between $\overline{\lambda}$ and λ_+, resulting in $\lambda_+ = 2\overline{\lambda}$.

A further confirmation of such link is obtained by exploiting the alignment property of $\boldsymbol{\xi}$, following which the Lyapunov vectors tend to align the direction of the maximum growth rate of ρ [15].

In order to compare the proposed statistics with the average energy cascade effects, $\overline{\lambda}$ and λ_+ are expressed in terms of the longitudinal velocity correlation function $f = \langle u_r u_r' \rangle / u^2$, where $u^2 = 1/3 \langle \mathbf{u} \cdot \mathbf{u} \rangle$, $u_r = \mathbf{u}(t, \mathbf{x}) \cdot \mathbf{r}/r$, and $u_r' = \mathbf{u}(t, \mathbf{x} + \mathbf{r}) \cdot \mathbf{r}/r$. This relationship leads to the closure formulas of von Kármán–Howarth and Corrsin equations and coincides with that just presented in [1], where the author adopts only λ_+ and $\overline{\lambda}$ without considering the distribution of the local exponents. There, the proposed closure formula leads to a value of the skewness of $\partial u_r / \partial r$ equal to $-3/7$, in agreement with those obtained by the several authors with direct numerical simulation of the Navier–Stokes equations (DNS) [16–18] and Large–eddy simulations (LES) [19–21]. Therefore, the here proposed statistics should be adequate for describing the distribution of $\widetilde{\lambda}$, at least for what concerns the main properties of the energy cascade phenomenon. The novelty of this work with respect to the literature and in particular with respect to [1] is represented by the statistics of $\widetilde{\lambda}$ and its distribution function. This latter provides much more detailed statistical information about the energy cascade and viscous dissipation than the analysis of [1] which, adopting average exponents, describes only the mean effects. The present analysis provides, by means of such PDF, the estimation of all the Lyapunov exponent statistical moments. Accordingly, this study recovers, among the other things, the results of [1] and, in addition, gives all the statistical properties arising from this specific PDF, in particular, the deviations of such effects of dissipation and energy cascade with respect to their average values.

Furthermore, to justify the hypotheses of the proposed statistics, the theoretical results of this latter are compared with numerical simulations of a proper differential system representing the incompressible fluid kinematics.

2. Interval of Variation of $\widetilde{\lambda}$ in Incompressible Turbulence

This section proposes an analysis for estimating the range of variations of $\widetilde{\lambda}$ based on the hypotheses of fluid incompressibility and fully developed chaos.

The present analysis starts from the consideration that the turbulent energy cascade is related to the fluid particles trajectories divergence; therefore the relative fluid kinematics plays an important role in the estimation of the properties of such energy cascade [1, 2]. The relative kinematics is expressed by finite scale Lyapunov vector $\boldsymbol{\xi}$ which satisfies

$$\begin{aligned} \dot{\mathbf{x}} &= \mathbf{u}(t, \mathbf{x}), \\ \dot{\boldsymbol{\xi}} &= \mathbf{u}(t, \mathbf{x} + \boldsymbol{\xi}) - \mathbf{u}(t, \mathbf{x}), \end{aligned} \tag{3}$$

where $\mathbf{u} = \mathbf{u}(t, \mathbf{x})$ varies according to the Navier–Stokes equations and $\mathbf{x}(t)$ and $\mathbf{y}(t) = \mathbf{x}(t) + \boldsymbol{\xi}(t)$ are two fluid

particles trajectories. The local divergence between $\mathbf{x}(t)$ and $\mathbf{y}(t)$ is quantified by $\widetilde{\lambda}$ which, due to the bifurcations of the kinematic field (kinematic bifurcations), exhibits oscillations of sizable amplitude with respect to its average value. These bifurcations continuously happen in those points of the space where

$$\det\left(\nabla \mathbf{u}\left(t, \mathbf{x}\right)\right) = 0. \tag{4}$$

Observe that the kinematic bifurcations defined by (4) are not the Navier–Stokes equations bifurcations (dynamic bifurcation) but arise from these latter [2]. In fact, the Navier–Stokes bifurcations frequently occur determining continuously nonsmooth spatial variations of $\mathbf{u}(t, \mathbf{x})$ which in turn lead to condition (4) in the several points of the space.

The definition of $\widetilde{\lambda}$ given by (1) implies that $\boldsymbol{\xi}$ can be locally expressed as

$$\boldsymbol{\xi} = \mathbf{Q}\left(t\right)\boldsymbol{\xi}\left(0\right)\exp\left(\widetilde{\lambda}t\right), \tag{5}$$

where $\widetilde{\lambda}$ plays the role of the stochastic variable and $\mathbf{Q}(t)$ is a proper orthogonal matrix providing the orientation of $\boldsymbol{\xi}$ with respect to the inertial frame $\mathscr{R}$. Accordingly, $\dot{\boldsymbol{\xi}}$ is

$$\dot{\boldsymbol{\xi}} = \widetilde{\lambda}\boldsymbol{\xi} + \boldsymbol{\omega} \times \boldsymbol{\xi} \tag{6}$$

in which $\boldsymbol{\omega}$ defines the angular velocity of $\boldsymbol{\xi}$ with respect to $\mathscr{R}$.

For an assigned velocity field, finite scale Lyapunov exponents and vectors are formally calculated with (1) through the following orthogonalization procedure: (a) the maximal local Lyapunov exponent, say $\widetilde{\lambda}_1$, is first obtained by choosing the direction $\mathbf{e}_1(t) \equiv \boldsymbol{\xi}_1/|\boldsymbol{\xi}_1|$ which maximizes $\widetilde{\lambda}$ in (1), (b) the second exponent $\widetilde{\lambda}_2 \leq \widetilde{\lambda}_1$ is calculated by selecting the direction $\mathbf{e}_2(t) \equiv \boldsymbol{\xi}_2/|\boldsymbol{\xi}_2|$ in the subspace (plane) orthogonal to $\boldsymbol{\xi}_1$ which maximizes $\widetilde{\lambda}$, and (c) finally, the third one $\widetilde{\lambda}_3 \leq \widetilde{\lambda}_2 \leq \widetilde{\lambda}_1$ corresponds to the direction $\mathbf{e}_3 \equiv \boldsymbol{\xi}_3/|\boldsymbol{\xi}_3|$ normal to both $\mathbf{e}_1$ and $\mathbf{e}_2$, where $|\boldsymbol{\xi}_1| = |\boldsymbol{\xi}_2| = |\boldsymbol{\xi}_3|$. The so obtained vectors system $E \equiv (\mathbf{e}_1, \mathbf{e}_2, \mathbf{e}_3)$ defines a rigid space which moves with respect to $\mathscr{R}$ with a given angular velocity $\boldsymbol{\omega}_E$ depending on the local fluid motion. Therefore, $\boldsymbol{\xi}_k$ and $\widetilde{\lambda}_k$, $k = 1, 2, 3$, are locally expressed by

$$\begin{aligned} \boldsymbol{\xi}_k &= \mathbf{Q}\left(t\right)\boldsymbol{\xi}_k\left(0\right)\exp\left(\widetilde{\lambda}_k t\right), \\ \dot{\boldsymbol{\xi}}_k &= \widetilde{\lambda}_k\boldsymbol{\xi}_k + \boldsymbol{\omega}_E \times \boldsymbol{\xi}_k, \\ & \qquad k = 1, 2, 3. \end{aligned} \tag{7}$$

The classical local Lyapunov exponents $\widetilde{\Lambda}_k$ are defined for $\boldsymbol{\xi}_k \to 0$, $k = 1, 2, 3$.

Now, in order to estimate the set of variations of $\widetilde{\lambda}$, observe that, due to fluid incompressibility, $\nabla \cdot \mathbf{u} \equiv 0$ and the classical local exponents obey to the following condition:

$$\widetilde{\Lambda}_1 + \widetilde{\Lambda}_2 + \widetilde{\Lambda}_3 = 0. \tag{8}$$

In general, (8) does not hold for finite scale Lyapunov vectors. Nevertheless, (8) is valid for those finite scale vectors for which the volume $\boldsymbol{\xi}_1 \times \boldsymbol{\xi}_2 \cdot \boldsymbol{\xi}_3$ is locally preserved: therefore, without lack of generality, these exponents can be written in the form

$$\begin{aligned} \widetilde{\lambda}_1 &= \lambda_m \cos\left(\varepsilon\right), \\ \widetilde{\lambda}_2 &= \lambda_m \cos\left(\varepsilon + \frac{2}{3}\pi\right), \\ \widetilde{\lambda}_3 &= \lambda_m \cos\left(\varepsilon + \frac{4}{3}\pi\right), \end{aligned} \tag{9}$$

where ε and λ_m are variables depending on the current act of motion and

$$\widetilde{\lambda}_1 + \widetilde{\lambda}_2 + \widetilde{\lambda}_3 = 0, \quad \widetilde{\lambda}_1 \geq \widetilde{\lambda}_2 \geq \widetilde{\lambda}_3. \tag{10}$$

Now, following the hypothesis of fully developed chaos, it is reasonable that $\widetilde{\lambda}$ ranges in the set (λ_0, λ_S), where $\lambda_S > 0$ assumes its maximum value compatible with (9) and λ_0 is consequently calculated. This implies that $\lambda_0 = -\lambda_S/2$, that is,

$$\begin{aligned} \widetilde{\lambda} &\in \left(-\frac{\lambda_S}{2}, \lambda_S\right), \\ \lambda_S &= \sup\left\{\lambda_m\right\}. \end{aligned} \tag{11}$$

It is worth remarking that λ_S depends on the instantaneous velocity field which in turn is the result of time evolution of the fluid motion starting from the initial condition following the Navier–Stokes equations. Hence, at the current time, λ_S assumes values related to viscous dissipation and kinetic energy both consequence of the fluid motion.

3. Incompressible Fully Developed Turbulence

This section studies the distribution functions $P = P(t, \mathbf{x}, \boldsymbol{\xi})$ and $P_\lambda = P_\lambda(t, \widetilde{\lambda})$ in incompressible fully developed turbulence, where $P(t, \mathbf{x}, \boldsymbol{\xi})$ and $P_\lambda(t, \widetilde{\lambda})$ are, respectively, the distribution functions of fluid particles position and Lyapunov vector and of local Lyapunov exponent. In particular, we will show that the proposed statistics leads to the following relations:

$$\begin{aligned} \left\langle \widetilde{\lambda} \right\rangle &= \frac{\lambda_+}{2}, \\ \left\langle \widetilde{\lambda}^2 \right\rangle &= \lambda_+^2 \end{aligned} \tag{12}$$

and to the link between λ_+ and the longitudinal velocity correlation function.

According to (1), P_λ depends on P and is expressed in terms of this latter through the Frobenius–Perron equation

$$P_\lambda\left(t, \widetilde{\lambda}\right) = \int_{\mathbf{x}}\int_{\xi} P\left(t, \mathbf{x}, \boldsymbol{\xi}\right)\delta\left(\widetilde{\lambda} - \frac{\dot{\boldsymbol{\xi}} \cdot \boldsymbol{\xi}}{\boldsymbol{\xi} \cdot \boldsymbol{\xi}}\right) d\mathbf{x}\, d\boldsymbol{\xi}, \tag{13}$$

where δ is the Dirac's delta. Hence, the distribution function P is first studied. This PDF changes with the time according to

the Liouville theorem [22] associated with (3). This theorem, arising from the relation

$$\int_{\mathbf{x}}\int_{\xi} P\, d\mathbf{x}\, d\boldsymbol{\xi} = 1, \quad \forall t > 0 \tag{14}$$

and from (3), provides the evolution equation of P [22]

$$\frac{\partial P}{\partial t} + \nabla_{\mathbf{x}} \cdot (P\dot{\mathbf{x}}) + \nabla_{\xi} \cdot \left(P\dot{\boldsymbol{\xi}}\right) = 0, \tag{15}$$

where $\nabla_{\mathbf{x}} \cdot (\circ)$ and $\nabla_{\xi} \cdot (\circ)$ denote the divergence of $(\circ)$ defined in the spaces $\{\mathbf{x}\}$ and $\{\boldsymbol{\xi}\}$ respectively and $d\mathbf{x}$ and $d\boldsymbol{\xi}$ are the elemental volumes in the corresponding spaces.

Taking into account (14) and that the homogeneous isotropic turbulence is defined for unbounded fluid domains, P will satisfy the following boundary condition:

$$P = 0, \quad \forall (\mathbf{x}, \boldsymbol{\xi}) \in \partial \{\{\mathbf{x}\} \times \{\boldsymbol{\xi}\}\} \equiv \partial \{\mathbf{x}\} \cup \partial \{\boldsymbol{\xi}\}. \tag{16}$$

Accordingly, the statistical average of an integrable function of $\mathbf{x}$ and $\boldsymbol{\xi}$, say ζ, is calculated in terms of P

$$\langle \zeta \rangle = \int_{\mathbf{x}}\int_{\xi} P\zeta\, d\mathbf{x}\, d\boldsymbol{\xi}. \tag{17}$$

In particular, average and maximum finite scale Lyapunov exponents are

$$\left\langle \widetilde{\lambda} \right\rangle = \int_{\mathbf{x}}\int_{\xi} P(t, \mathbf{x}, \boldsymbol{\xi}) \frac{\dot{\boldsymbol{\xi}} \cdot \boldsymbol{\xi}}{\boldsymbol{\xi} \cdot \boldsymbol{\xi}} d\mathbf{x}\, d\boldsymbol{\xi} \equiv \int_{\lambda} P_{\lambda}\left(t, \widetilde{\lambda}\right) \widetilde{\lambda}\, d\widetilde{\lambda}, \tag{18}$$

$$\begin{aligned} \lambda_{+} &= \frac{\int_{\mathbf{x}} \int_{\dot{\xi}\cdot\xi \geq 0} P(t, \mathbf{x}, \boldsymbol{\xi}) \left(\left(\dot{\boldsymbol{\xi}} \cdot \boldsymbol{\xi}\right) / (\boldsymbol{\xi} \cdot \boldsymbol{\xi})\right) d\mathbf{x}\, d\boldsymbol{\xi}}{\int_{\mathbf{x}} \int_{\dot{\xi}\cdot\xi \geq 0} P(t, \mathbf{x}, \boldsymbol{\xi})\, d\mathbf{x}\, d\boldsymbol{\xi}} \\ &= \frac{\int_{\widetilde{\lambda} \geq 0} P_{\lambda}\left(t, \widetilde{\lambda}\right) \widetilde{\lambda}\, d\widetilde{\lambda}}{\int_{\widetilde{\lambda} \geq 0} P_{\lambda}\left(t, \widetilde{\lambda}\right) d\widetilde{\lambda}}. \end{aligned} \tag{19}$$

Remark 1. It is very important to observe that the Liouville theorem in the form of (15) holds also when the variable velocity field is replaced with the same field frozen at the current time. This is due to the hypothesis that the times of variations of the velocity field, which changes according to the Navier–Stokes equations, are much larger than those associated with $\mathbf{x}$ and $\boldsymbol{\xi}$ whose times of variations are of the order of $1/\widetilde{\lambda}$. Following such hypothesis, the statistics of $\mathbf{x}$ and $\boldsymbol{\xi}$ does not depend on the time variations of $\mathbf{u}$ and can be considered to be the result of the instantaneous fluid act of motion.

3.1. Distribution Function of $\mathbf{x}$ *and* $\boldsymbol{\xi}$. For the sake of our convenience, we introduce the quantity $\mathbf{y} \equiv (\mathbf{x}, \boldsymbol{\xi}) \in \mathscr{A} \subset \{\mathbf{y}\}$ which defines the relative kinematics, being $\{\mathbf{y}\} \equiv \{\mathbf{x}\} \times \{\boldsymbol{\xi}\}$; thus the Liouville theorem reads as

$$\frac{\partial P}{\partial t} + \nabla_{\mathbf{y}} \cdot (P\mathbf{f}) = 0, \tag{20}$$

where

$$\dot{\mathbf{y}} = \mathbf{f}(\mathbf{y}) \equiv (\mathbf{u}(t, \mathbf{x}), \mathbf{u}(t, \mathbf{x} + \boldsymbol{\xi}) - \mathbf{u}(t, \mathbf{x})). \tag{21}$$

Now, the entropy $\mathscr{H}$ associated with $\mathbf{y}$ is defined as

$$\mathscr{H}(P) = -\int_{\mathbf{x}}\int_{\xi} P \ln P\, d\mathbf{x}\, d\boldsymbol{\xi} \equiv -\int_{\mathbf{y}} P \ln P\, d\mathbf{y}. \tag{22}$$

Due to fluid incompressibility, $\nabla_{\mathbf{y}} \cdot \mathbf{f} \equiv 0$; therefore from the Liouville theorem the entropy rate identically vanishes

$$\frac{d\mathscr{H}}{dt} = \int_{\mathbf{y}} P \nabla_{\mathbf{y}} \cdot \mathbf{f}\, d\mathbf{y} \equiv 0. \tag{23}$$

In order to estimate the steady distribution of $\mathbf{y}$, observe that the fully developed turbulence corresponds to a situation of maximum chaos where the kinematic bifurcations cause a total loss of the initial condition data of $\mathbf{y}$. Accordingly, it is reasonable that $\mathscr{H}$ assumes its maximum value compatible with (14) and (20) where $\partial P/\partial t = 0$. This corresponds to the following variational problem:

$$J = \int_{\mathbf{y}} \mathscr{L}\, d\mathbf{y} = \max, \tag{24}$$

in which

$$\mathscr{L}\left(P, \nabla_{\mathbf{y}} P\right) = -P \ln P + \eta P + \chi \nabla_{\mathbf{y}} \cdot (P\mathbf{f}) \tag{25}$$

is the Lagrangian of the problem and η and $\chi = \chi(\mathbf{y})$ are the Lagrange multipliers associated with conditions (14) and (20), respectively. The maximum of J is then obtained as steady condition for J ($\delta J = 0$) through the variational calculus and this leads to the Euler–Lagrange equation

$$\frac{\partial \mathscr{L}}{\partial P} - \nabla_{\mathbf{y}} \cdot \left(\frac{\partial \mathscr{L}}{\partial \nabla_{\mathbf{y}} P}\right) = 0 \tag{26}$$

whose solutions are searched for substituting (25) into (26)

$$P = A \exp\left(\nabla_{\mathbf{y}} \chi \cdot \mathbf{f}\right), \tag{27}$$

where A is the normalization constant related to η whose value is calculated with (14), whereas $\chi(\mathbf{y})$ is obtained through the Liouville equation. This latter gives

$$\nabla_{\mathbf{y}} \cdot \left((\mathbf{f} \otimes \mathbf{f}) \nabla_{\mathbf{y}} \chi\right) = 0 \tag{28}$$

in which $(\circ \otimes \circ)$ denotes the dyadic product between vectors. Integrating (28), we obtain

$$(\mathbf{f} \otimes \mathbf{f}) \nabla_{\mathbf{y}} \chi = \boldsymbol{\Phi}(\mathbf{y}), \tag{29}$$

where $\boldsymbol{\Phi}$ is an arbitrary solenoidal vector field. Now, the determinant of $(\mathbf{f} \otimes \mathbf{f})$ identically vanishes; thus (29) admits solutions only for $\boldsymbol{\Phi} \equiv 0$. Moreover, as $(\mathbf{f} \otimes \mathbf{f})$ exhibits minimum rank, (29) has only the trivial solution

$$\nabla_{\mathbf{y}} \chi = 0, \quad \forall \mathbf{y} \in \mathscr{A} \subset \{\mathbf{y}\} \tag{30}$$

i.e., $\mathbf{y}$ is uniformly distributed on $\mathscr{A} \subset \{\mathbf{y}\}$, being

$$P = \begin{cases} \dfrac{1}{m\{\mathscr{A}\}}, & \forall \mathbf{y} \in \mathscr{A} \subset \{\mathbf{y}\} \\ 0 & \text{elsewhere} \end{cases} \tag{31}$$

in which $m\{\circ\}$ indicates the measure of the set $\circ$.

3.2. Lyapunov Exponents Distribution Function. In order to estimate P_λ, the following should be noted.

If $\widetilde{\lambda}$ is given, (1) corresponds to a hypersurface $\Sigma_{\widetilde{\lambda}}$ of the space $\{\mathbf{y}\}$ whose equation reads as

$$\Sigma_{\widetilde{\lambda}} : G\left(\mathbf{y};\widetilde{\lambda}\right) \equiv -\widetilde{\lambda} + \frac{\dot{\boldsymbol{\xi}}\left(\mathbf{x},\boldsymbol{\xi}\right)\cdot\boldsymbol{\xi}}{\boldsymbol{\xi}\cdot\boldsymbol{\xi}} = 0. \tag{32}$$

When $\widetilde{\lambda}$ varies, $\Sigma_{\widetilde{\lambda}}$ and its points $\mathbf{y}_* \equiv (\mathbf{x}_*, \boldsymbol{\xi}_*)$ will change according to (32)

$$\frac{d\mathbf{y}_*}{d\widetilde{\lambda}} = \frac{\mathbf{n}}{\left|\nabla_{\mathbf{y}} G\right|} + \beta\boldsymbol{\tau}, \tag{33}$$

where $\mathbf{n} \equiv \nabla_{\mathbf{y}} G/|\nabla_{\mathbf{y}} G|$ and $\boldsymbol{\tau}$ are, respectively, local normal and tangent unit vectors to $\Sigma_{\widetilde{\lambda}}$ both calculated in $\mathbf{y}_*$, being $\beta\boldsymbol{\tau}$ not determined. On the other hand, $d\mathbf{y}_*/d\widetilde{\lambda}$ can be determined considering that $\mathbf{x}_*$ does really not depend on $\widetilde{\lambda}$, whereas the variations of $\boldsymbol{\xi}_*$ are related to those of $\widetilde{\lambda}$ by means of (5) and (6). Thus, $d\mathbf{y}_*/d\widetilde{\lambda}$ is locally expressed as

$$\frac{d\mathbf{y}_*}{d\widetilde{\lambda}} \equiv \left(\mathbf{0}, \frac{d\boldsymbol{\xi}_*}{d\widetilde{\lambda}}\right) = \left(\mathbf{0}, \frac{t}{\widetilde{\lambda}}\left(\dot{\boldsymbol{\xi}} - \omega\times\boldsymbol{\xi}\right)\right). \tag{34}$$

As $\dot{\boldsymbol{\xi}}$ is solenoidal, the surface integrals of $d\mathbf{y}_*/d\widetilde{\lambda}\cdot\mathbf{n}$ over arbitrary hypersurfaces $\Sigma_{\widetilde{\lambda}}$ (flow of $d\mathbf{y}_*/d\widetilde{\lambda}$ through $\Sigma_{\widetilde{\lambda}}$) assume the same value which does not depend on $\widetilde{\lambda}$, i.e.,

$$\int_{\Sigma_{\widetilde{\lambda}_1}} \left(\frac{d\mathbf{y}_*}{d\widetilde{\lambda}}\right)\cdot\mathbf{n}\, d\sigma = \int_{\Sigma_{\widetilde{\lambda}_2}} \left(\frac{d\mathbf{y}_*}{d\widetilde{\lambda}}\right)\cdot\mathbf{n}\, d\sigma, \qquad \forall\widetilde{\lambda}_1,\widetilde{\lambda}_2 \in \left(-\frac{\lambda_S}{2},\lambda_S\right) \tag{35}$$

Therefore, from (33), we obtain

$$\int_{\Sigma_{\widetilde{\lambda}_1}} \frac{d\sigma}{\left|\nabla_{\mathbf{y}} G\right|} = \int_{\Sigma_{\widetilde{\lambda}_2}} \frac{d\sigma}{\left|\nabla_{\mathbf{y}} G\right|}, \quad \forall\widetilde{\lambda}_1,\widetilde{\lambda}_2 \in \left(-\frac{\lambda_S}{2},\lambda_S\right). \tag{36}$$

Now, the distribution function of $\widetilde{\lambda}$ is calculated substituting (31) into the Frobenius–Perron equation (13) and considering that $\mathbf{y}$ is uniformly distributed on $\mathscr{A}$

$$\begin{aligned} P_\lambda\left(\widetilde{\lambda}\right) &= \int_{\mathbf{y}} P\left(\mathbf{y}\right)\delta\left(G\left(\mathbf{y};\widetilde{\lambda}\right)\right)d\mathbf{y} \\ &= \frac{1}{m\left(\mathscr{A}\right)}\int_{\mathscr{A}} \delta\left(G\left(\mathbf{y};\widetilde{\lambda}\right)\right)d\mathbf{y} \\ &= \frac{1}{m\left(\mathscr{A}\right)}\int_{\Sigma_\lambda} \frac{d\sigma}{\left|\nabla_{\mathbf{y}} G\right|}, \end{aligned} \tag{37}$$

where the surface integral over $\Sigma_\lambda \subset \mathscr{A}$, described by $G(\mathbf{y};\widetilde{\lambda}) = 0$, is formally calculated according to the Minkowski measure theory [23]. Taking into account (36) and that $\widetilde{\lambda} \in (-\lambda_S/2, \lambda_S)$, $\widetilde{\lambda}$ results to be uniformly distributed in $(-\lambda_S/2, \lambda_S)$, being

$$P_\lambda = \begin{cases} \dfrac{2}{3}\dfrac{1}{\lambda_S}, & \text{if } \widetilde{\lambda} \in \left(-\dfrac{\lambda_S}{2},\lambda_S\right) \\ 0 & \text{elsewhere.} \end{cases} \tag{38}$$

Hence, $\overline{\lambda}$ and λ_+ are calculated in terms of P_λ with (18) and (19)

$$\begin{aligned} \overline{\lambda} &\equiv \left\langle\widetilde{\lambda}\right\rangle = \frac{\lambda_S}{4} > 0, \\ \lambda_+ &\equiv \left\langle\widetilde{\lambda}\right\rangle_{\dot{\xi}\cdot\xi\geq 0} = \frac{\lambda_S}{2} = 2\left\langle\widetilde{\lambda}\right\rangle. \end{aligned} \tag{39}$$

Next, it is useful to calculate the mean square $\langle\widetilde{\lambda}^2\rangle$

$$\left\langle\widetilde{\lambda}^2\right\rangle = \int_{-\lambda_S/2}^{\lambda_S} P_\lambda\widetilde{\lambda}^2\, d\widetilde{\lambda} = \lambda_+^2. \tag{40}$$

According to (40), the mean square of $\widetilde{\lambda}$ equals the square of the average of $\widetilde{\lambda}$ calculated for $\dot{\boldsymbol{\xi}}\cdot\boldsymbol{\xi} \geq 0$, and the standard deviation is proportional to $\langle\widetilde{\lambda}\rangle$

$$\sigma = \sqrt{\left\langle\widetilde{\lambda}^2\right\rangle - \left\langle\widetilde{\lambda}\right\rangle^2} = \sqrt{3}\left\langle\widetilde{\lambda}\right\rangle = \frac{\sqrt{3}}{4}\lambda_S. \tag{41}$$

It is worth remarking that the obtained distribution (38) is the result of three effects, of which two are in competition with each other. The first one of these, due to the Lyapunov vectors tendency to align the maximum growth rate direction of ρ, is responsible for variation intervals in which $\widetilde{\lambda} > 0$, producing trajectories instability. The second one, related to the fluid incompressibility, acts in opposite sense preserving the volume, determining regions where $\widetilde{\lambda} < 0$. The third element is the chaotic regime, here given by imposing $\mathscr{H} = \max$, which causes a continuous distribution of $\widetilde{\lambda} \in (-\lambda_S/2, \lambda_S)$.

4. Analysis through Alignment Property of $\boldsymbol{\xi}$

One reasonable confirmation of the previous results is here given by exploiting the alignment property of $\boldsymbol{\xi}$, following which $\boldsymbol{\xi}$ tends to align with the direction of the maximum growth rate of ρ [15] and the fluid incompressibility. This leads to an alternative way to achieve (12). Accordingly, λ_+ is now calculated adopting a proper PDF $P_+ = P_+(t,\mathbf{x},\boldsymbol{\xi})$ obtained as projection of $P(t,\mathbf{x},\boldsymbol{\xi})$ at the time $t+\tau$, where $\mathbf{x}$ is considered to be constant and τ is the Lyapunov time defined by

$$\frac{d\ln\rho}{dt} = \frac{\langle\ln\rho\rangle - \ln\rho}{\tau}. \tag{42}$$

After the time τ, the alignment tendency of $\boldsymbol{\xi}$ provides the fact that mostly all the Lyapunov vectors calculated at $\mathbf{x} = \text{const}$ will be such that $\dot{\boldsymbol{\xi}}\cdot\boldsymbol{\xi} \geq 0$. The vectors lying in subspaces of $\{\boldsymbol{\xi}\}$ orthogonal to the maximum rising rate direction of ρ which do not follow such alignment form a null measure set in $\{\mathbf{y}\}$; thus P_+ is a distribution function which satisfies

$$\begin{aligned} &\forall\left(\mathbf{x},\boldsymbol{\xi}\right) \in \{\mathbf{x}\}\times\{\boldsymbol{\xi}\} \mid \dot{\boldsymbol{\xi}}\cdot\boldsymbol{\xi} \geq 0 \;\; P_+\left(t,\mathbf{x},\boldsymbol{\xi}\right) > 0, \\ &\forall\left(\mathbf{x},\boldsymbol{\xi}\right) \in \{\mathbf{x}\}\times\{\boldsymbol{\xi}\} \mid \dot{\boldsymbol{\xi}}\cdot\boldsymbol{\xi} < 0 \;\; P_+\left(t,\mathbf{x},\boldsymbol{\xi}\right) = 0 \end{aligned} \tag{43}$$

and is expressed in function of P and τ

$$\begin{aligned} P_+\left(t,\mathbf{x},\boldsymbol{\xi}\right) &= P\left(t,\mathbf{x},\boldsymbol{\xi} + \dot{\boldsymbol{\xi}}\tau + O\left(\tau^2\right)\right) \\ &= P + \nabla_\xi P\cdot\dot{\boldsymbol{\xi}}\tau + O\left(\tau^2\right), \end{aligned} \tag{44}$$

where $P = P(t, \mathbf{x}, \boldsymbol{\xi})$ and $\nabla_\xi P = \nabla_\xi P(t, \mathbf{x}, \boldsymbol{\xi})$. Neglecting the higher order terms, P_+ is calculated as

$$P_+ = P + \nabla_\xi P \cdot \dot{\boldsymbol{\xi}} \tau. \tag{45}$$

This PDF identically satisfies (14). In fact, the integral over $\{\mathbf{x}\} \times \{\boldsymbol{\xi}\}$ of the first term at the RHS of (45) is equal to one, whereas the integral of the second one can be reduced to a proper surface integral of P over $\partial\{\boldsymbol{\xi}\}$, where $P \equiv 0$ through Green's identity; thus this identically vanishes. Furthermore P_+ exhibits the same entropy of P at least of higher order terms, which in turn does not vary with the time due to the fluid incompressibility

$$\begin{aligned} \mathscr{H}(P_+) &= -\int_{\mathbf{x}} \int_{\xi} P_+ \ln P_+ \, d\mathbf{x}\, d\boldsymbol{\xi} \\ &= \mathscr{H}(P) - \tau \int_{\mathbf{x}} \int_{\xi} \nabla_\xi P \cdot \dot{\boldsymbol{\xi}} (1 + \ln P) \, d\mathbf{x}\, d\boldsymbol{\xi} \\ &\quad + O\left(\tau^2\right). \end{aligned} \tag{46}$$

The second addend at the RHS of (46) identically vanishes as it can be reduced to be a surface integral of P over $\partial\{\boldsymbol{\xi}\}$, where $P \equiv 0$. Therefore

$$\mathscr{H}(P_+) = \mathscr{H}(P) + O\left(\tau^2\right). \tag{47}$$

At the least higher order terms, P_+ maintains the same level of information of P; thus it is adequate to estimate λ_+. Accordingly, this latter is calculated as

$$\lambda_+ = \int_{\mathbf{x}} \int_{\xi} P_+(t, \mathbf{x}, \boldsymbol{\xi}) \frac{\dot{\boldsymbol{\xi}} \cdot \boldsymbol{\xi}}{\boldsymbol{\xi} \cdot \boldsymbol{\xi}} d\mathbf{x}\, d\boldsymbol{\xi}. \tag{48}$$

Substituting (45) and (42) into (48), we have

$$\lambda_+ = \left\langle \widetilde{\lambda} \right\rangle - \int_{\mathbf{x}} \int_{\xi} \nabla_\xi P \cdot \dot{\boldsymbol{\xi}} \left(\ln \rho - \langle \ln \rho \rangle\right) d\mathbf{x}\, d\boldsymbol{\xi}. \tag{49}$$

Integrating by parts the second addend and taking into account the fluid incompressibility and the boundary conditions (16), we obtain

$$\begin{aligned} &\int_{\mathbf{x}} \int_{\xi} \nabla_\xi P \cdot \dot{\boldsymbol{\xi}} \left(\ln \rho - \langle \ln \rho \rangle\right) d\mathbf{x}\, d\boldsymbol{\xi} \\ &\quad = -\int_{\mathbf{x}} \int_{\xi} P \frac{\dot{\boldsymbol{\xi}} \cdot \boldsymbol{\xi}}{\boldsymbol{\xi} \cdot \boldsymbol{\xi}} d\mathbf{x}\, d\boldsymbol{\xi} \equiv -\left\langle \widetilde{\lambda} \right\rangle. \end{aligned} \tag{50}$$

Hence

$$\lambda_+ = 2 \left\langle \widetilde{\lambda} \right\rangle \tag{51}$$

in agreement with previous results.

5. Lyapunov Exponents in Terms of Longitudinal Velocity Correlation

The results of the previous analysis allow achieving the link between λ_+ and the longitudinal velocity correlation function. In fact, the standard deviation of longitudinal velocity difference directly depends on u^2 and f according to

$$\left\langle \left(u_r' - u_r\right)^2 \right\rangle = 2u^2 \left(1 - f(r)\right). \tag{52}$$

On the other hand, the Lyapunov theory gives the longitudinal velocity difference in terms of $\widetilde{\lambda}$

$$u_r' - u_r = \widetilde{\lambda} \left(\boldsymbol{\xi} \cdot \frac{\boldsymbol{\xi}}{|\boldsymbol{\xi}|} \right)_{\boldsymbol{\xi} = \mathbf{r}}. \tag{53}$$

Taking into account the isotropy and (40), $\langle (u_r' - u_r)^2 \rangle$ reads as

$$\left\langle \left(u_r' - u_r\right)^2 \right\rangle \equiv \left\langle \dot{r}^2 \right\rangle = \left\langle \widetilde{\lambda}^2 \right\rangle r^2 = \lambda_+^2 r^2, \tag{54}$$

thus, $\lambda_+ = \lambda_+(r)$ and $\overline{\lambda} = \overline{\lambda}(r)$ are expressed in function of the finite scale r by means of the longitudinal velocity correlation f

$$\overline{\lambda}(r) = \frac{\lambda_+(r)}{2} = \frac{u}{r} \sqrt{\frac{1 - f(r)}{2}}. \tag{55}$$

Equation (55) coincides with that proposed in [1] which leads to the closure formulas of the von Kármán and Corrsin equations. Unlike [1], (55) is here achieved exploiting the shape of the distribution (38). Reference [1] shows that (55) provides a value of the skewness of $\partial u_r/\partial r$ equal to $\langle (\partial u_r/\partial r)^3 \rangle / \langle (\partial u_r/\partial r)^2 \rangle^{3/2} = -3/7 = -0.428\ldots$ (see the appendix), in good agreement with the results obtained by the several authors with direct numerical simulation of the Navier–Stokes equations (DNS) [16–18] ($-0.47 \div -0.40$) and Large–eddy simulations (LES) [19–21] ($-0.42 \div -0.40$). In detail, Table 1 recalls the comparison between the value of the skewness

$$H_3(0) = \frac{\left\langle \left(\partial u_r/\partial r\right)^3 \right\rangle}{\left\langle \left(\partial u_r/\partial r\right)^2 \right\rangle^{3/2}} \tag{56}$$

calculated with the proposed analysis and those obtained by the aforementioned works. As a result the maximum absolute difference between the proposed value and the other ones is less than 10%. Furthermore, other studies [24–26] have shown that the closure formulas referable to this analysis

Table 1: Comparison of the results: skewness of $\partial u_r/\partial r$ at diverse Taylor scale Reynolds number $R_T \equiv u\lambda_T/\nu$ following different authors.

Reference	Simulation	R_T	$H_3(0)$
Present analysis	-	-	$-3/7 = -0.428...$
[16]	DNS	202	−0.44
[17]	DNS	45	−0.47
[18]	DNS	64	−0.40
[19]	LES	<71	−0.40
[20]	LES	∞	−0.40
[21]	LES	720	−0.42

provide kinetic energy and temperature spectra which exhibit scaling laws in agreement with the theoretical arguments of Kolmogorov, Obukov–Corrsin, and Batchelor [27–29]. Therefore, the adopted hypothesis $\mathscr{H} = \max$ and the consequent distribution (38) seem to be adequate assumptions at least for what concerns the estimation of turbulent energy cascade main effects.

6. Results and Discussions

In order to justify the plausibility of the previous hypotheses, this section presents one statistical analysis of numerical simulations of a simple differential system representing incompressible fluid kinematics. This system is properly chosen in such a way that it can exhibit simple mathematical structure and chaotic behavior corresponding to an expected high value of entropy $\mathscr{H}$. To achieve this latter condition, we adopt an adequate differential system which shows a "weak" or "reduced" link between velocity and spatial coordinates and an expected huge number of bifurcations per unit time (bifurcations rate). For this reason, each velocity component is assumed to be depending only on one single spatial coordinate with opportune scaling factors. Thus, the chosen differential system is given by

$$\begin{aligned} \frac{dx}{dt} &= u = \sin z, \quad x(0) = x_0 \\ \frac{dy}{dt} &= v = \frac{\sin qx}{q}, \quad y(0) = y_0 \\ \frac{dz}{dt} &= w = \frac{\sin q^2 y}{q^2}, \quad z(0) = z_0, \end{aligned} \tag{57}$$

where q, giving different scaling factors along the coordinate directions, will be properly selected to study the system behavior and to obtain a high bifurcations rate. The velocity field is periodic and $\mathscr{C} \equiv (0, 2\pi/q) \times (0, 2\pi/q^2) \times (0, 2\pi)$ represents the smallest regions of periodicity. The velocity gradient is then

$$\nabla_{\mathbf{x}}\mathbf{u} = \begin{bmatrix} 0 & 0 & \cos z \\ \cos qx & 0 & 0 \\ 0 & \cos q^2 y & 0 \end{bmatrix} \tag{58}$$

and its determinant, $\det(\nabla_{\mathbf{x}}\mathbf{u}) = \cos qx \cos q^2 y \cos z$, vanishes in those points, where at least one of qx, $q^2 y$, and z assumes values $\pi(1/2 \pm k)$, $k = 0, 1, 2, \ldots$. Accordingly, large values of bifurcations rate are expected when q is opportunely high. Observe that, due to its peculiar analytical structure, the system generates trajectories which can differ from isotropic turbulence, while it is not sure that $\mathscr{H}$ assumes its maximum value. Nevertheless, as its Jacobian determinant vanishes in numerous points, it is reasonable that the proposed system shows a high entropy and a behavior which can be in some way compared to the fully developed chaos. Hence, although the regime $\mathscr{H} = \max$ and (57) can correspond to different PDFs, say P_λ and $P_{\lambda E}$, respectively, it is reasonable that the two distributions show elements in common, especially for what concerns the interval where $\widetilde{\lambda}$ ranges. In particular, according to this analysis, we would expect

$$\begin{aligned} I_1 &= \int_{-\lambda_S/2}^{\lambda_S} P_{\lambda E}\, d\widetilde{\lambda} \lesssim 1, \\ I_2 &= \frac{\int_{-\infty}^{0} P_{\lambda E}\, d\widetilde{\lambda}}{\int_{0}^{\infty} P_{\lambda E}\, d\widetilde{\lambda}} \approx \frac{1}{2}, \\ \frac{\overline{\lambda}}{\lambda_+} &\approx \frac{1}{2}, \\ \frac{\sigma}{\overline{\lambda}} &\approx \sqrt{3}, \end{aligned} \tag{59}$$

where I_1, I_2, $\overline{\lambda}/\lambda_+$, and $\sigma/\overline{\lambda}$ are statistical parameters related to the PDF shape. Following (59), it is plausible that the occurrences $\widetilde{\lambda} > 0$ are about two times those $\widetilde{\lambda} < 0$ and that most of the occurrences of $\widetilde{\lambda}$ happen in $(-\lambda_S/2, \lambda_S)$, where λ_S is here obtained in function of $\langle\widetilde{\lambda}\rangle_E$ by means of (39) and (40), i.e.,

$$\lambda_S = 4\left\langle\widetilde{\lambda}\right\rangle_E \tag{60}$$

being $\langle\widetilde{\lambda}\rangle_E$ the average of $\widetilde{\lambda}$ calculated through $P_{\lambda E}$. Moreover, λ_+ and σ are expected to be proportional to $\overline{\lambda}$, with $\overline{\lambda}/\lambda_+$ and $\sigma/\overline{\lambda}$ satisfying (59).

The results, here presented by two sets of eight cases, are obtained by means of numerical simulations. Tables 2 and 3 report the mentioned statistic parameters, and Figures 1 and 2 show the distribution functions for different values of q.

Table 2: Statistical parameters for $|\boldsymbol{\xi}| = 10^{-7}$.

q	$\overline{\lambda}$	I_1	I_2	$\overline{\lambda}/\lambda_+$	$\sigma/\overline{\lambda}$
2.75	0.1879	0.9095	0.4210	0.5339	1.7426
3.75	0.2067	0.9483	0.3726	0.5823	1.5411
4.50	0.1739	0.9003	0.4345	0.5224	1.7981
17.00	0.04525	0.9823	0.5360	0.4859	1.7472
17.50	0.04805	0.9747	0.5197	0.4945	1.8267
19.25	0.04220	0.9897	0.5356	0.4988	1.6693
20.75	0.03970	0.9839	0.5077	0.4994	1.7948
24.00	0.03262	0.9910	0.5593	0.4785	1.7630

Table 3: Statistical parameters for $|\boldsymbol{\xi}| = 10^{-3}$.

q	$\overline{\lambda}$	I_1	I_2	$\overline{\lambda}/\lambda_+$	$\sigma/\overline{\lambda}$
2.75	0.1945	0.9173	0.3998	0.5473	1.7007
3.75	0.2026	0.9442	0.3822	0.5739	1.5740
4.50	0.1685	0.8912	0.4509	0.5081	1.8610
17.00	0.04804	0.9067	0.5103	0.4542	2.3244
17.50	0.05202	0.9358	0.4816	0.4983	2.0231
19.25	0.04448	0.9200	0.5344	0.4555	2.2818
20.75	0.04111	0.9168	0.5150	0.4534	2.3871
24.00	0.03466	0.9176	0.5299	0.4475	2.4426

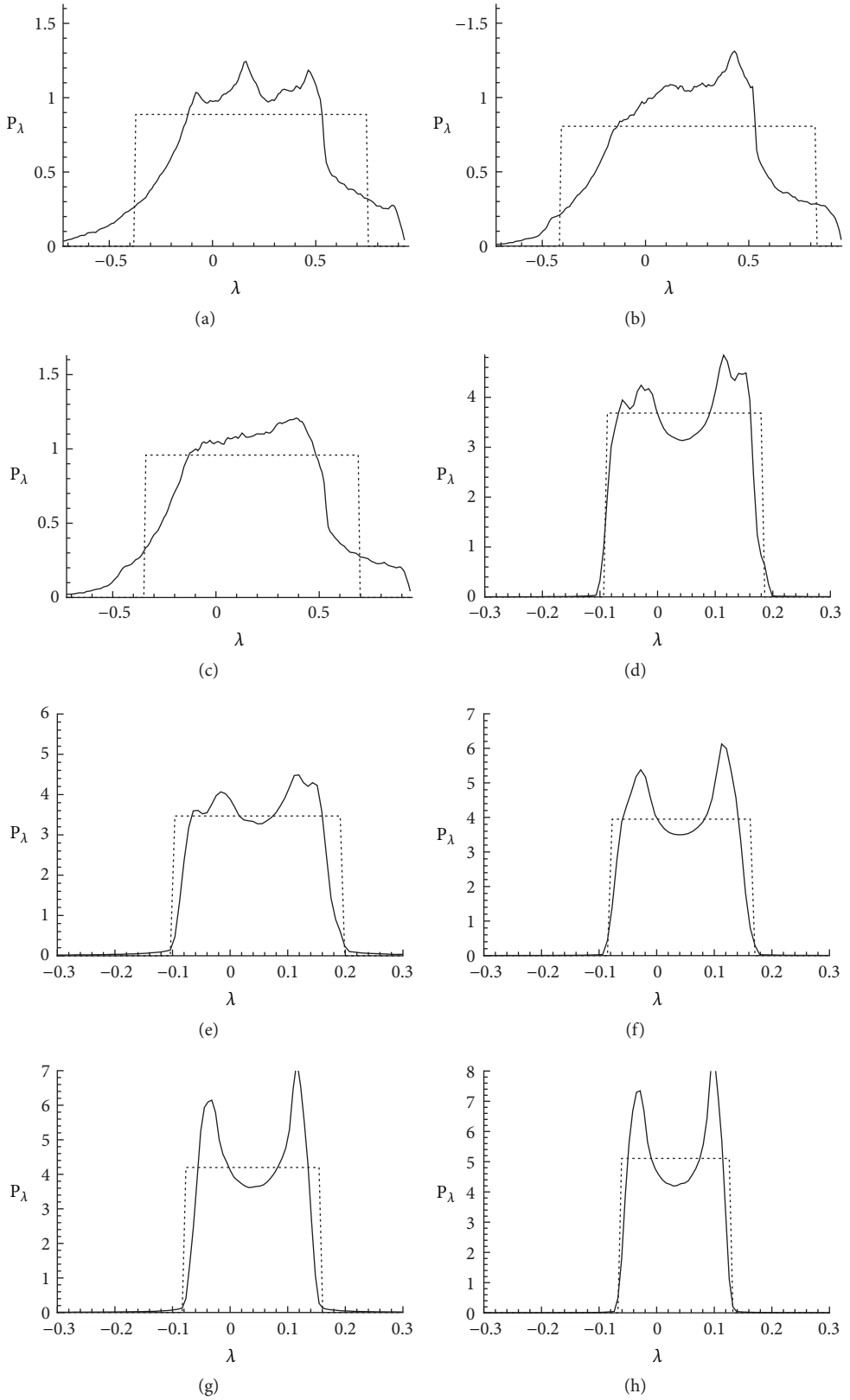

FIGURE 1: Distribution function of $\widetilde{\lambda}$ for $|\boldsymbol{\xi}| = 10^{-7}$. (a) $q = 2.75$, (b) $q = 3.75$, (c) $q = 4.5$, (d) $q = 17$, (e) $q = 17.5$, (f) $q = 19.25$, (g) $q = 20.75$, and (h) $q = 24$.

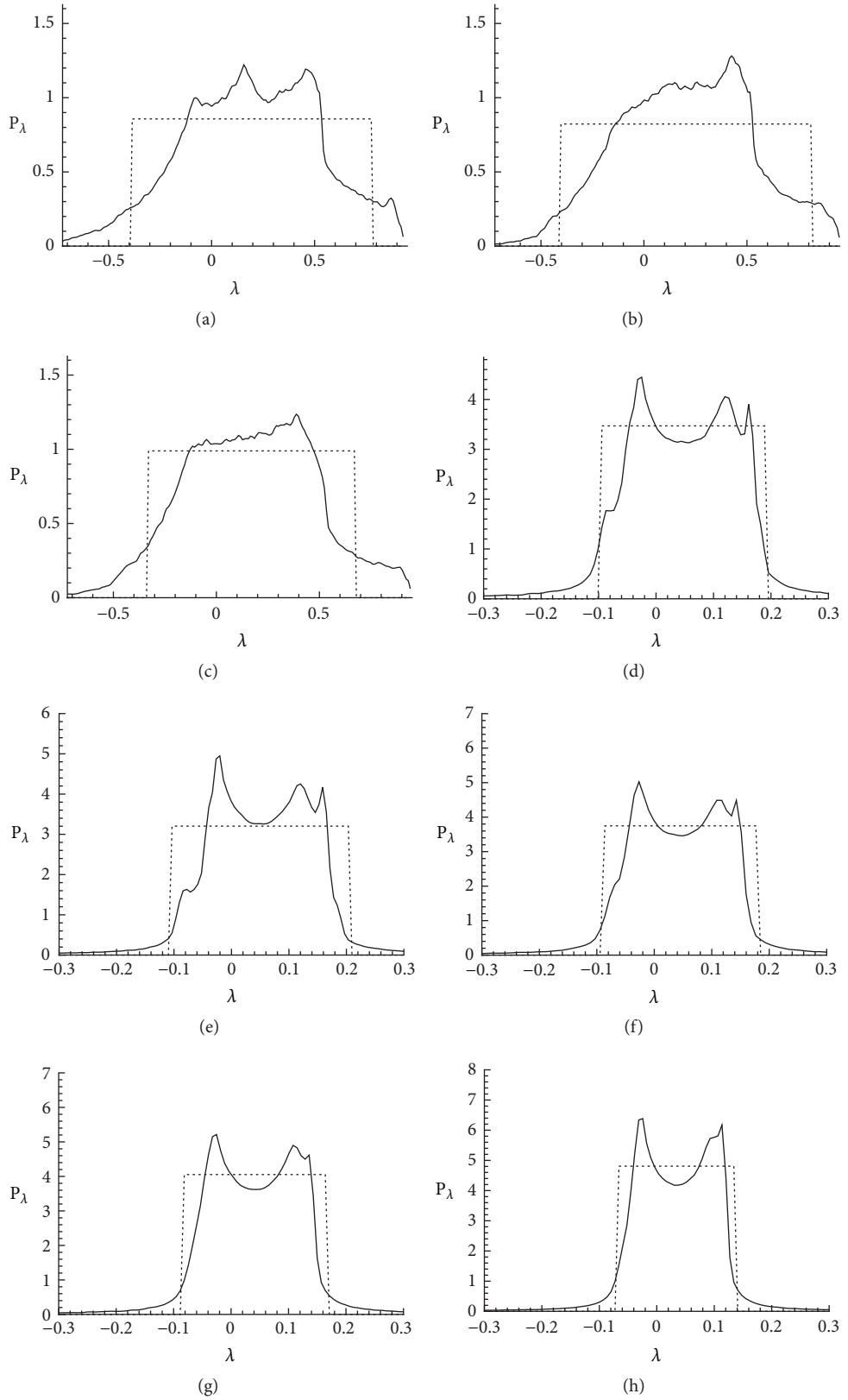

FIGURE 2: Distribution function of $\widetilde{\lambda}$ for $|\boldsymbol{\xi}| = 10^{-3}$. (a) $q = 2.75$, (b) $q = 3.75$, (c) $q = 4.5$, (d) $q = 17$, (e) $q = 17.5$, (f) $q = 19.25$, (g) $q = 20.75$, and (h) $q = 24$.

The set of differential equations is given by (57) and by the corresponding evolution equations of $\boldsymbol{\xi}$ following (3). During the process of integration, the Lyapunov vectors are continuously rescaled (at each time step) in order to maintain the initial scale $|\boldsymbol{\xi}(0)|$ at which $\boldsymbol{\xi}$ and $\widetilde{\lambda}$ are both referred to. The scheme of integration is a fourth-order Runge–Kutta method with automatic adaptive step size, which returns equidistant samples $\mathbf{x}(t_k)$, $\boldsymbol{\xi}(t_k)$, and $t_k = k\Delta t$, $k = 1, 2, \ldots, N$, with Δt properly computed. Specifically, the time of integration is assumed to be $T = 30000/\widetilde{\lambda}_{0\max}$, with $\widetilde{\lambda}_{0\max}$ the maximum Lyapunov exponent at $t = 0$ and $N = 2 \cdot 10^6$. Thereafter, the distribution functions of $\widetilde{\lambda}$ are numerically computed through statistical elaboration of the simulations data. In order to obtain an expected high value of the bifurcations rate, the assumed values of q are such that $q \in (2, 25)$. For what concerns the initial conditions, all the simulations are computed for $x_0 = 0.1$, $y_0 = 0.2$, and $z_0 = 0.3$, with an initial orientation of $\boldsymbol{\xi}$ corresponding to the minimum rising rate of ρ.

In line with the chaotic trajectories behaviors, we selected the simulations where $\mathbf{x}$ describes almost completely at least $\mathscr{C}$, or at least the union of regions of space equivalent to $\mathscr{C}$. The first set of simulations, obtained for $|\xi| = 10^{-7}$, is reported in Figure 1, and the other one, depicted in Figure 2, is computed for $|\xi| = 10^{-3}$. Solid and dotted lines represent, respectively, $P_{\lambda E}$ and the estimates of P_λ obtained from (38) and (60). It is apparent that although the two PDFs differ from each other, the computed values of $\widetilde{\lambda}$ are unsymmetrically distributed in such a way that I_1 and I_2, standard deviation and exponents ratio satisfy the relations (59). In particular, σ is proportional to $\overline{\lambda}$ in any case with a proportionality constant around to $\sqrt{3}$ $(0.8 \div 2.5)$.

We conclude this section by observing that variations of q and of initial conditions in terms of position $\mathbf{x}(0)$ and/or orientation of $\boldsymbol{\xi}(0)$ can produce change in the shape of $P_{\lambda E}$ and of the aforementioned parameters, depending on how the system describes its phase space. In particular, if $\mathbf{x}$ sweeps almost completely at least $\mathscr{C}$—or at least the union of regions of $\{\mathbf{x}\}$ equivalent to $\mathscr{C}$—$\widetilde{\lambda}$ is found to be unsymmetrically distributed and the values of I_1, I_2, $\sigma/\overline{\lambda}$, and $\overline{\lambda}/\lambda_+$ agree with those given in (59). On the contrary, in the cases where $\mathbf{x}$ only partially sweeps $\mathscr{C}$—or the equivalent union of parts of space—sizable differences can be observed with respect to the present results in terms of PDF shape and statistical parameters.

7. Conclusions

The distribution function of the finite scale local Lyapunov exponent of the kinematic field was studied in homogeneous isotropic turbulence. Based on reasonable assumptions regarding the fully developed chaos and the fluid incompressibility, the shape of such distribution and the range of variations of $\widetilde{\lambda}$ are determined. This distribution results in an uniform function in a proper nonsymmetric interval of variations. The results arising from such PDF, in particular the link between λ_+ and $\overline{\lambda}$ and the closure for the longitudinal velocity correlation equation, agree with those presented in [1], and this should support the hypothesis $\mathscr{K} = \max$. An alternative way to determine the link between such exponents is also presented, which is based on the alignment property of the Lyapunov vectors. Direct simulations of a very simple differential system representing incompressible fluid kinematics give results which corroborate the hypotheses of the present analysis.

Appendix

This appendix reports some of the results dealing with the closure of the von Kármán–Howarth equation, obtained in [1, 25].

For fully developed isotropic homogeneous turbulence, the longitudinal velocity correlation function

$$f(r) = \frac{\langle u_r(\mathbf{x})\, u_r(\mathbf{x}+\mathbf{r})\rangle}{u^2} \tag{A.1}$$

obeys the von Kármán–Howarth equation [11]

$$\frac{\partial f}{\partial t} = \frac{K(r)}{u^2} + 2\nu\left(\frac{\partial^2 f}{\partial r^2} + \frac{4}{r}\frac{\partial f}{\partial r}\right) + \frac{10\nu}{\lambda_T^2} f \tag{A.2}$$

the boundary conditions of which are

$$\begin{aligned} f(0) &= 1, \\ \lim_{r\to\infty} f(r) &= 0, \end{aligned} \tag{A.3}$$

where ν is the fluid kinematic viscosity and $u \equiv \sqrt{\langle u_r^2(\mathbf{x})\rangle}$ follows the kinetic energy equation obtained from (A.2) for $r \to 0$ [11]

$$\frac{du^2}{dt} = -\frac{10\nu}{\lambda_T^2} u^2 \tag{A.4}$$

being $\lambda_T \equiv \sqrt{-1/f''(0)}$ the Taylor scale. The quantity $K(r)$ gives the energy cascade, being linked to the longitudinal triple velocity correlation function k

$$\begin{aligned} K(r) &= u^3\left(\frac{\partial}{\partial r} + \frac{4}{r}\right) k(r), \\ &\text{where } k(r) = \frac{\langle u_r^2(\mathbf{x})\, u_r(\mathbf{x}+\mathbf{r})\rangle}{u^3}. \end{aligned} \tag{A.5}$$

Thus, the von Kármán–Howarth equation gives the relationship between the statistical moments $\langle(\Delta u_r)^2\rangle$ and $\langle(\Delta u_r)^3\rangle$ in function of r.

The analysis in [1, 25] provides the closure of the von Kármán–Howarth equation and expresses $K(r)$ in terms of longitudinal velocity correlation

$$K(r) = u^3\sqrt{\frac{1-f}{2}}\frac{\partial f}{\partial r}. \tag{A.6}$$

The skewness of Δu_r is [30]

$$H_3(r) \equiv \frac{\left\langle (\Delta u_r)^3 \right\rangle}{\left\langle (\Delta u_r)^2 \right\rangle^{3/2}} = \frac{6k(r)}{\left(2\left(1 - f(r)\right)\right)^{3/2}}. \quad (A.7)$$

Therefore, the skewness of $\partial u_r/\partial r$ is

$$H_3(0) = -\frac{3}{7}. \quad (A.8)$$

Data Availability

The obtained results in this manuscript are supported by theoretical and numerical data available from Professor Nicola de Divitiis, "La Sapienza" University, Dipartimento di Ingegneria Meccanica e Aerospaziale, via Eudossiana, 18, 00184, Rome, Italy.

Disclosure

This work received no specific grant from any funding agency in the public, commercial, or not-for-profit sectors.

Conflicts of Interest

The author declares that there are no conflicts of interest regarding the publication of this article.

Acknowledgments

This work was partially supported by the Italian Ministry for the Universities and Scientific and Technological Research (MIUR).

References

[1] N. de Divitiis, "von Kármán–Howarth and Corrsin equations closure based on Lagrangian description of the fluid motion," *Annals of Physics*, vol. 368, pp. 296–309, 2016.

[2] N. de Divitiis, "Bifurcations analysis of turbulent energy cascade," *Annals of Physics*, vol. 354, pp. 604–617, 2015.

[3] M. K. Baev and G. G. Chernykh, "On Corrsin equation closure," *Journal of Engineering Thermophysics*, vol. 19, no. 3, pp. 154–169, 2010.

[4] V. N. Grebenev and M. Oberlack, "A Chorin-type formula for solutions to a closure model for the von Kármán-Howarth equation," *Journal of Nonlinear Mathematical Physics*, vol. 12, no. 1, pp. 1–9, 2005.

[5] K. Hasselmann, "Zur Deutung der dreifachen Geschwindigkeitskorrelationen der isotropen Turbulenz," *Deutsche Hydrographische Zeitschrift*, vol. 11, no. 5, pp. 207–217, 1958.

[6] J. A. Domaradzki and G. L. Mellor, "A simple turbulence closure hypothesis for the triple-velocity correlation functions in homogeneous isotropic turbulence," *Journal of Fluid Mechanics*, vol. 140, pp. 45–61, 1984.

[7] M. Millionshtchikov, "Isotropic turbulence in the field of turbulent viscosity," *JETP Letters*, vol. 8, pp. 406–411, 1969.

[8] M. Oberlack and N. Peters, "Closure of the two-point correlation Equation as a basis for Reynolds stress models," *Applied Scientific Research*, vol. 51, no. 1-2, pp. 533–538, 1993.

[9] F. Thiesset, R. A. Antonia, L. Danaila, and L. Djenidi, "Kármán-Howarth closure equation on the basis of a universal eddy viscosity," *Physical Review E: Statistical, Nonlinear, and Soft Matter Physics*, vol. 88, no. 1, Article ID 011003(R), 2013.

[10] M. Cencini and A. Vulpiani, "Finite size Lyapunov exponent: review on applications," *Journal of Physics A: Mathematical and General*, vol. 46, no. 25, Article ID 254019, 26 pages, 2013.

[11] T. von Kármán and L. Howarth, "On the Statistical Theory of Isotropic Turbulence," *Proceedings of the Royal Society of London. Series A, Mathematical and Physical Sciences*, vol. 164, no. 917, pp. 192–215, 1938.

[12] S. Corrsin, "The decay of isotropic temperature fluctuations in an isotropic turbulence," *Journal of Aeronautical Science*, vol. 18, no. 12, pp. 417–423, 1951.

[13] S. Corrsin, "On the spectrum of isotropic temperature fluctuations in an isotropic turbulence," *Journal of Applied Physics*, vol. 22, no. 4, pp. 469–473, 1951.

[14] J. M. Ottino, "Mixing, chaotic advection, and turbulence," *Annual Review of Fluid Mechanics*, vol. 22, no. 1, pp. 207–253, 1990.

[15] E. Ott, *Chaos in Dynamical Systems*, Cambridge University Press, Cambridge, UK, 2nd edition, 2002.

[16] S. Chen, G. D. Doolen, R. H. Kraichnan, and Z.-S. She, "On statistical correlations between velocity increments and locally averaged dissipation in homogeneous turbulence," *Physics of Fluids*, vol. 5, no. 2, pp. 458–463, 1992.

[17] S. A. Orszag and G. S. Patterson, "Numerical simulation of three-dimensional homogeneous isotropic turbulence," *Physical Review Letters*, vol. 28, no. 2, pp. 76–79, 1972.

[18] R. Panda, V. Sonnad, E. Clementi, S. A. Orszag, and V. Yakhot, "Turbulence in a randomly stirred fluid," *Physics of Fluids A. Fluid Dynamics*, vol. 1, no. 6, pp. 1045–1053, 1989.

[19] R. Anderson and C. Meneveau, "Effects of the similarity model in finite-difference LES of isotropic turbulence using a Lagrangian dynamic mixed model," *Flow, Turbulence and Combustion*, vol. 62, no. 3, pp. 201–225, 1999.

[20] D. Carati, S. Ghosal, and P. Moin, "On the representation of backscatter in dynamic localization models," *Physics of Fluids*, vol. 7, no. 3, pp. 606–616, 1995.

[21] H. S. Kang, S. Chester, and C. Meneveau, "Decaying turbulence in an active-grid-generated flow and comparisons with large-eddy simulation," *Journal of Fluid Mechanics*, vol. 480, pp. 129–160, 2003.

[22] G. Nicolis, *Introduction to Nonlinear Science*, Cambridge University Press, Cambridge, UK, 1995.

[23] H. Federer, *Geometric Measure Theory*, Springer, Berlin, Germany, 1969.

[24] N. de Divitiis, "Finite scale Lyapunov analysis of temperature fluctuations in homogeneous isotropic turbulence," *Applied Mathematical Modelling: Simulation and Computation for Engineering and Environmental Systems*, vol. 38, no. 21-22, pp. 5279–5297, 2014.

[25] N. de Divitiis, "Lyapunov analysis for fully developed homogeneous isotropic turbulence," *Theoretical and Computational Fluid Dynamics*, vol. 25, no. 6, pp. 421–445, 2011.

[26] N. de Divitiis, "Self-similarity in fully developed homogeneous isotropic turbulence using the lyapunov analysis," *Theoretical and Computational Fluid Dynamics*, vol. 26, no. 1-4, pp. 81–92, 2012.

[27] A. M. Obuhov, "The structure of the temperature field in a turbulent flow," *Doklady Akademii Nauk*, vol. 13, p. 391, 1949.

[28] G. K. Batchelor, "Small-scale variation of convected quantities like temperature in turbulent fluid. I. General discussion and the case of small conductivity," *Journal of Fluid Mechanics*, vol. 5, pp. 113–133, 1959.

[29] G. K. Batchelor, I. D. Howells, and A. A. Townsend, "Small-scale variation of convected quantities like temperature in turbulent fluid Part 2. The case of large conductivity," *Journal of Fluid Mechanics*, vol. 5, no. 1, pp. 134–139, 1959.

[30] G. Batchelor, *The Theory of Homogeneous Turbulence*, Cambridge University Press, Cambridge, UK, 1953.